

A van Hemmen-Kondo model for disordered strongly correlated electron systems.

S. G. Magalhaes^a, F. M. Zimmer^a, B. Coqblin^b

^a*Departamento de Física, Universidade Federal de Santa Maria,
Santa Maria 97105-900, RS, Brazil*

^b*L.P.S., CNRS UMR 8502, Université Paris-Sud,
91405-Orsay, France*

Abstract

We present here a theoretical model in order to describe the competition between the Kondo effect and the spin glass behavior. The spin glass part of the starting Hamiltonian contains Ising spins with an intersite exchange interaction given by the local van Hemmen model, while the Kondo effect is described as usual by the intrasite exchange J_K . We obtain, for large J_K values, a Kondo phase and, for smaller J_K values, a succession, with decreasing temperature, of a spin glass phase, a mixed spin glass-ferromagnetic one and finally a ferromagnetic phase. This model improves the theoretical description of disordered Kondo systems with respect to previous models and can account for experimental data in Cerium disordered systems like $CeCu_{1-x}Ni_x$ alloys.

1 Introduction

The interplay between disorder and strong electronic correlations is recognized as a very interesting issue in condensed matter physics. There are now many experimental evidences showing the very important role of the disorder in f -electron systems in addition to the RKKY or Kondo interactions [1]. As a result, it can appear complex phase diagrams which show spin glass (SG) phases in addition to the onset of antiferromagnetism (AF) or ferromagnetism (FE), regions dominated by the Kondo effect, the presence of Quantum Phase Transitions (QPT) and exotic regions which present non-Fermi liquid behavior (NFL) [2].

Earlier experimental results can illustrate the mentioned complexity. For instance, in $CeAu_{1-x}Co_xSi_3$ alloys [3], when Au is replaced by Co , it first appears a SG phase, then there is the onset of an AF phase with the Néel temperature decreasing towards a Quantum Critical Point (QCP). Thus, the glassy behaviour tends to decrease with the increase of x and finally, for $x > 0.9$, there is a complete screening of magnetic moments due to the Kondo effect.

More recently, experimental findings in $CePd_{1-x}Rh_x$ [4, 5] and $CeNi_{1-x}Cu_x$ [6, 7] have enlarged the set of non-trivial behaviour in disordered f -electron systems. In both systems, there are strong indications that a glassy behaviour is

present in a suitable range of doping and this behaviour has been recently identified to appear as a cluster glass state. In the well studied $CeNi_{1-x}Cu_x$ case, the Kondo interaction is dominating for x smaller than approximately 0.2 [8]. However, the intermediate doping regime has been extensively studied both experimentally and theoretically and finally a complex scenario is obtained when the temperature is decreased. In the first experimental studies on $CeNi_{1-x}Cu_x$ alloys with x typically between 0.3 and 0.6, a SG phase has been obtained below the paramagnetic state and then there is a transition to a ferromagnetic phase at lower temperatures.

More sophisticated experiments have recently shown that dynamic magnetic clusters are developing at low temperatures below the paramagnetic state. More precisely, there is the formation of clusters due to short range ferromagnetic correlations below a certain temperature T^* . The volume fraction of these clusters increases as temperature is lowered and they become frozen at T_{cl} well below T^* and, therefore, it appears an inhomogeneous ferromagnetic order at very low temperatures [6, 7]. Thus, there is a change, below the paramagnetic phase, from a cluster spin glass to a disordered ferromagnetic order without any sharp transition, but with a mixed and disordered intermediate phase.

A Kondo-Cluster-Glass state has been also recently evidenced in $CePd_{1-x}Rh_x$ alloys at very low temperatures. This system exhibits a continuous evolution from a ferromagnetic order in $CePd$, with a Curie temperature $T_c = 6.6K$, to an intermediate-valence ground state in $CeRh$. The Curie temperature decreases continuously with increasing x and tends to 25 mK at the value $x = 0.87$. Despite pronounced non-Fermi-liquid behavior in the proximity of this concentration for specific heat and thermal expansion, it was concluded from the analysis of the Gruneisen ratio that there is no QCP [9]. On the opposite, a “Kondo-cluster-glass” state was found for x larger than 0.65: there is firstly the formation of clusters with predominantly ferromagnetic couplings of the f -moments below a given temperature T^* and then a random freezing of the cluster moments below a smaller temperature T_{cl} [4, 5]. Thus, there are clearly similarities between the low temperature behaviors of $CeNi_{1-x}Cu_x$ and $CePd_{1-x}Rh_x$ alloys, but both a more profound analysis of the different data and the role of the Kondo effect have to be precised in these two systems.

Several theoretical studies have tried, since already some time, to account for the previous experimental data. A Kondo lattice with an additional Ising term and a random coupling between localized spins, called here the Kondo-Ising Lattice (KIL) model [10, 11, 12], has been firstly used to study the competition between the Kondo effect and magnetism when disorder is present within the Static Approximation (SA) [13]. It appears that, for $CeAu_{1-x}Co_xSi_3$ alloys, a Gaussian random distributed bond would be adequate as can be seen in Refs. [12, 14]. The same model has been also firstly used to describe the case of $CeNi_{1-x}Cu_x$ alloys, where the disorder has been introduced within the classical Sherrington-Kirkpatrick (SK) model [15] by taking Gaussian random intersite coupling J_{ij} with a mean value J_0 different from zero to describe the ferromagnetic ordering [11]. The phase diagram giving the temperature T versus the strength J_K of the Kondo interaction has been computed and we have obtained, besides the Kondo state, magnetic phases like Spin Glass (SG), Ferromagnetic (FE) and a mixed phase (SG+FE). For this particular solution, the ferromagnetic order occurs with replica symmetry breaking. This phase diagram could be, therefore, a good starting point to describe the scenario found

in $CeNi_{1-x}Cu_x$ alloys. Unfortunately, for this particular kind of disorder, the Curie temperature T_c is always higher than the freezing one, which is a scenario opposite to the experimental situation observed in $CeNi_{1-x}Cu_x$ system.

Thus, in order to solve the preceding difficulty, a completely different perspective has been adopted in reference [16]. The theoretical description of the disorder has been modified from a bond disordered coupling to a site disordered one. In that case, the J_{ij} coupling is a generalization of the Mattis model [17] used extensively to study complex systems [18], given as $J_{ij} = \frac{J}{2N} \sum_{\mu=1}^p \xi_i^\mu \xi_j^\mu$, where ξ_i^μ is a random variable which follows a bimodal distribution.

One important aspect is that, in the corresponding mean field approach using such J_{ij} values, it is possible to introduce a parameter which allows to control the level of frustration in the problem [16]. The first interesting result is that the Kondo solution is robust in the large J_K limit, no matter what is the level of frustration. For weak frustration and small J_K , below a certain temperature, it appears a SG solution. When the temperature is further decreased, the SG solution is replaced by Mattis states which have the same thermodynamics as a FE phase [18]. This result suggests that the situation found in $CeNi_{1-x}Cu_x$ alloys would be an example of weak frustration. Nevertheless, there is an important difference between this model and the approach of the Gaussian distributed J_{ij} . For the kind of disorder given by this generalized Mattis model, there is no mixed phase solution for the order parameters, but on the contrary, there is a first order phase transition between the SG and Mattis states; such solutions can obviously coexist, but one of them is always metastable. In conclusion, our previous Mattis-like model gives the SG phase above the FE phase, but it cannot yield a real SG+FE mixed Phase [16].

Thus, in order to improve the preceding description and to have, therefore, a better agreement with experiment, we introduce here, in our previously used KIL model, a new kind of site disordered coupling J_{ij} , originally introduced by van Hemmen (vH) to study the Spin Glass in the classical Ising model [19]. The phase diagram obtained from such a classical model displays not only SG, FE+SG and FE phases, but also they can appear in that order when temperature is decreased. In this particular case, the SG+FE phase is characterized by both non zero magnetization and SG order parameters. Recently, a work [20] has studied a mean field solution of a quantum version of the vH model with an applied transverse field Γ and it shows that some aspects of its classical counterpart can still be preserved in the quantum vH model, and in particular the SG+FE phase. However, spin flipping introduced by the presence of Γ in the quantum vH model can modify the phase diagram, suppressing for instance the presence of SG+FE phase [20]. However, it is well known that an additional transverse field in the KIL model with a Gaussian random bond coupling between the localized Ising spins operators can produce important consequences as, for instance, a QCP [21].

In the present work, we will, therefore, study the KIL model with both the vH type of disorder for the intersite exchange interaction J_{ij} and a transverse field Γ which allows also to investigate the possible consequences for the phase diagram with the spin flipping. There is also another very important aspect related to the vH type of disorder introduced in the present work: in the previous approaches using the Gaussian random bond SK-type J_{ij} [10, 11, 12, 14, 21] or the site disorder type given by the product of random variables ξ_i^μ , the disorder-

der is treated using the so called replica symmetry solution for the SG order parameters [22]. This solution is well known to have a serious flaw, because it is locally unstable below the freezing temperature [23]. Certainly, that problem could be overcome by the use of replica symmetry breaking schemes [24]. However, this kind of scheme increases the number of order parameters in such a way that the search for order parameter solutions in the KIL model becomes extremely complicated. Nevertheless, that is not the only problem with the use of replicas to treat the disorder in the KIL model. There are also indications that the presence of one or other magnetic solutions could be dependent on the particular kind of replica symmetry breaking schemes [25]. By contrast, that is not the case for the disordered J_{ij} given in the vH model (see following equation (2)). The disorder can be treated without the use of replica technique as demonstrated in the classical and quantum vH models [19, 20]. Thus, the present use of the van Hemmen description of the disorder in the KIL model improves considerably the description of the Kondo-Spin glass-Ferromagnetism competition in disordered Kondo systems. It is important to remark that the present work is typically a mean field theory as in Refs. [10, 11, 12, 14, 21]. In particular, the Static and saddle point approximations are used here. The use of the first approximation can be justified since our goal is mainly to describe phase boundaries as discussed in Ref. [21]. The saddle point method is in fact exact here, as a consequence of the long range nature of the vH coupling.

This paper is structured as follows. In the next section, we introduce the model and calculate the corresponding thermodynamics. The following section is dedicated to discuss the numerical solutions of the saddle point equations for the order parameters and to derive the phase diagram. Finally, the last section is reserved to the conclusions.

2 General Formulation

The starting Hamiltonian in the KIL model is given by:

$$H = \sum_{ij,s} t_{ij} \hat{n}_{is}^d + \epsilon_0 \sum_{i,s} \hat{n}_{is}^f + J_K \sum_i [\hat{S}_{fi}^+ \hat{s}_{di}^- + \hat{S}_{fi}^- \hat{s}_{di}^+] - \sum_{i,j} J_{ij} \hat{S}_{fi}^z \hat{S}_{ji}^z - 2\Gamma \sum_i \hat{S}_{fi}^x. \quad (1)$$

In Eq. (1), $\hat{S}_{fi}^z = \frac{1}{2}[\hat{n}_{i\uparrow}^f - \hat{n}_{i\downarrow}^f]$, $\hat{S}_{fi}^+ = f_{i\uparrow}^\dagger f_{i\downarrow}$, $\hat{S}_{fi}^- = (\hat{S}_{fi}^+)^\dagger$, $\hat{S}_{fi}^x = f_{i\uparrow}^\dagger f_{i\downarrow} + f_{i\downarrow}^\dagger f_{i\uparrow}$, $\hat{s}_{di}^+ = d_{i\uparrow}^\dagger d_{i\downarrow}$, $\hat{s}_{di}^- = (\hat{s}_{di}^+)^\dagger$, $\hat{n}_{is}^f = f_{is}^\dagger f_{is}$, $\hat{n}_{is}^d = d_{is}^\dagger d_{is}$ where f_{is}^\dagger (f_{is}) and d_{is}^\dagger (d_{is}) are fermionic creation (destruction) operators of f and d electrons, respectively. The spin projections are indicated by $s = \uparrow$ or \downarrow .

The random coupling J_{ij} in Eq. (1) is given as in the vH model by:

$$J_{ij} = \frac{J}{N}(\xi_i \eta_j + \eta_i \xi_j) + \frac{J_0}{N} \quad (2)$$

where ξ_i and η_i in Eq. (2) are random variables which follow the bimodal distribution:

$$P(x) = \frac{1}{2}[\delta(x-1) + \delta(x+1)]. \quad (3)$$

In Eq. (3), $\delta(x)$ is the Dirac delta function. As discussed in the previous section, the coupling J_{ij} given in Eq. (2) is an infinite long range coupling which gives exact solutions in the thermodynamical limit for the saddle point approximation used below.

The partition function is expressed within functional formalism using anti-commuting Grassmann variables $\varphi_{is}(\tau)$ and $\psi_{is}(\tau)$ associated to the f and d electrons, respectively as [10, 21]:

$$Z = \int D(\psi^* \psi) D(\varphi^* \varphi) \exp [A_{VH} + A_K + A_0]. \quad (4)$$

In the static approximation (SA) [13] the actions in Eq (4) are given as:

$$A_0 = \sum_{\omega} \sum_{i,j} \left[(\underline{\psi})_i^\dagger(\omega) (i\omega - \beta\varepsilon_0 + \beta\Gamma \underline{\sigma}_x) \delta_{ij} \underline{\psi}_i(\omega) \right. \\ \left. + \underline{\varphi}_i^\dagger [(i\omega + \mu_d) \delta_{ij} - \beta t_{ij}] \underline{\varphi}_j(\omega) \right] \quad (5)$$

where, in the first term of Eq. (5), the chemical potential μ_f has been absorbed in ε_0 .

$$A_K^{stat} \approx \frac{J_K}{N} \sum_{is} \sum_{\omega} [\varphi_{i-s}^*(\omega) \psi_{i-s}(\omega)] \sum_{js} \sum_{\omega'} [\psi_{js}^*(\omega') \varphi_{js}(\omega')] , \quad (6)$$

$$A_{VH}^{stat} = \sum_{ij} J_{ij} S_{fi}^z S_{fj}^z \quad (7)$$

with

$$S_{fi}^z = \frac{1}{2} \sum_{\omega} \underline{\psi}_i^\dagger(\omega) \underline{\sigma}^z \underline{\psi}_i(\omega). \quad (8)$$

The action A_K^{stat} is given in the mean field approximation (see Ref [10]). In the remaining components of the action A_0 and A_{VH}^{stat} , spinors are used :

$$\underline{\varphi}_i(\omega) = \begin{pmatrix} \varphi_{i\uparrow}(\omega) \\ \varphi_{i\downarrow}(\omega) \end{pmatrix}, \quad \underline{\psi}_i(\omega) = \begin{pmatrix} \psi_{i\uparrow}(\omega) \\ \psi_{i\downarrow}(\omega) \end{pmatrix} \quad (9)$$

and the Pauli matrices are given as usual by:

$$\underline{\sigma}_x = \begin{pmatrix} 0 & 1 \\ 1 & 0 \end{pmatrix} \quad \underline{\sigma}_y = \begin{pmatrix} 0 & -i \\ i & 0 \end{pmatrix} \quad \underline{\sigma}_z = \begin{pmatrix} 1 & 0 \\ 0 & -1 \end{pmatrix}. \quad (10)$$

We follow a procedure close to that introduced in Ref. [10]. Therefore, the Kondo order parameter $\lambda_\sigma \approx \lambda = \frac{1}{N} \sum_{j,\omega} \langle \psi_{j\sigma}^*(\omega) \varphi_{i\sigma}(\omega) \rangle$ can be introduced in the partition function Z defined by Eqs. (4)-(8). Then, the φ fields are integrated and we obtain the following result:

$$Z/Z_d^0 = \exp(-2N\beta\lambda\lambda^*) Z_{eff} \quad (11)$$

where Z_d^0 is the partition function of free d electrons and

$$Z_{eff} = \int D(\psi^* \psi) \exp \left(A_{VH}^{stat} + \sum_{\omega\sigma} \sum_{i,j} \underline{\psi}_{i\sigma}^*(\omega) \underline{g}_{ij}^{-1}(\omega) \underline{\psi}_{j\sigma}(\omega) \right) \quad (12)$$

with

$$\underline{g}_{ij}^{-1}(\omega) = [(i\omega - \beta\epsilon_0)\underline{I} + \beta\Gamma\underline{\sigma}_z]\delta_{ij} - \frac{\beta^2 J_k^2 \lambda^2}{(i\omega + \mu_d)\delta_{ij} - \beta t_{ij}}\underline{I}. \quad (13)$$

In Eq.(13), we use the notation $|\lambda^2| \equiv \lambda^2$ and \underline{I} means the unitary matrix.

Introducing J_{ij} given by Eq. (2), the action A_{vH}^{stat} becomes composed of two terms: one randomic and the other one ferromagnetic. They can be rearranged to introduce SG and FE order parameters in Z_{eff} . The details of such calculations are shown in the Appendix.

The free energy is, therefore, given by:

$$\beta F = 2\beta J_K \lambda^2 - \lim_{N \rightarrow \infty} \frac{1}{N} \ln Z_{eff}. \quad (14)$$

Using the saddle point solution for Z_{eff} (see Eqs. ((24)-(25))), the free energy in Eq. (14) becomes:

$$\beta F = 2\beta J_K \lambda^2 + 2\beta J q_1 q_2 + \beta J_0 m^2 - \sum_{\omega} \ln(\det \underline{G}_{ij}^{-1}(\omega|h_j)). \quad (15)$$

The Green function $\underline{G}_{ij}^{-1}(\omega|h_j)$ is given in Eqs. (26)-(31). In order to proceed to the calculations, we use in the last term of Eq. (15) the approximation introduced in Ref. [10] which decouples the random magnetic field h_j from the Kondo lattice. Thus, we obtain:

$$\ln \det (\underline{G}_{ij}^{-1}(\omega|h_j)) \approx \frac{1}{N} \sum_j \ln [\det \underline{\Gamma}_{\mu\nu}^{-1}(\omega|h_j)] \quad (16)$$

with

$$\begin{aligned} \underline{\Gamma}_{\mu\nu}^{-1}(\omega|h_j) = & [(i\omega - \beta\epsilon_0)\underline{I} - \underline{\sigma}_z h_j + \beta\Gamma\underline{\sigma}_x] \delta_{\mu\nu} \\ & - \beta^2 J_k^2 \lambda^2 \frac{1}{N} \sum_{\vec{k}} \frac{e^{i\vec{k}\vec{R}_{\mu\nu}}}{(i\omega + \mu_d) - \beta\epsilon_k} \underline{I}. \end{aligned} \quad (17)$$

Now, in the last term of Eq. (15), we can use self-averaging property $\frac{1}{N} \sum_j f(\eta_j; \xi_j) = \langle \langle f(\eta; \xi) \rangle \rangle_{\xi\eta}$. Therefore:

$$\frac{1}{N} \sum_j \ln \left[\frac{1}{N} \sum_{\vec{k}} \left(\sum_{\omega} \Gamma_{\sigma}(\vec{k}, h_j) \right) \right] = \left\langle \left\langle \ln \left[\frac{1}{N} \sum_{\vec{k}} \left(\sum_{\omega} \Gamma_{\sigma}(\vec{k}, h) \right) \right] \right\rangle \right\rangle_{\xi\eta} \quad (18)$$

where

$$\langle \langle f(\xi, \eta) \rangle \rangle_{\xi\eta} = \int d\xi d\eta P(\xi, \eta) f(\xi, \eta) \quad (19)$$

Then, by assuming that $\mu_d = 0$ and $\epsilon_0 = 0$, the free energy can be found as

$$\begin{aligned} \beta F = & 2\beta J_k \lambda^2 + 2\beta J q_1 q_2 + \beta J_0 m^2 \\ & - \left\langle \left\langle \frac{1}{\beta D} \int_{-\beta D}^{+\beta D} dx \ln \left[\cosh \left(\frac{x + H}{2} \right) \right. \right. \right. \\ & \left. \left. \left. + \cosh \sqrt{\frac{1}{4}(x - H)^2 + \beta^2 J_k^2 \lambda^2} \right] \right\rangle \right\rangle_{\xi\eta} \end{aligned} \quad (20)$$

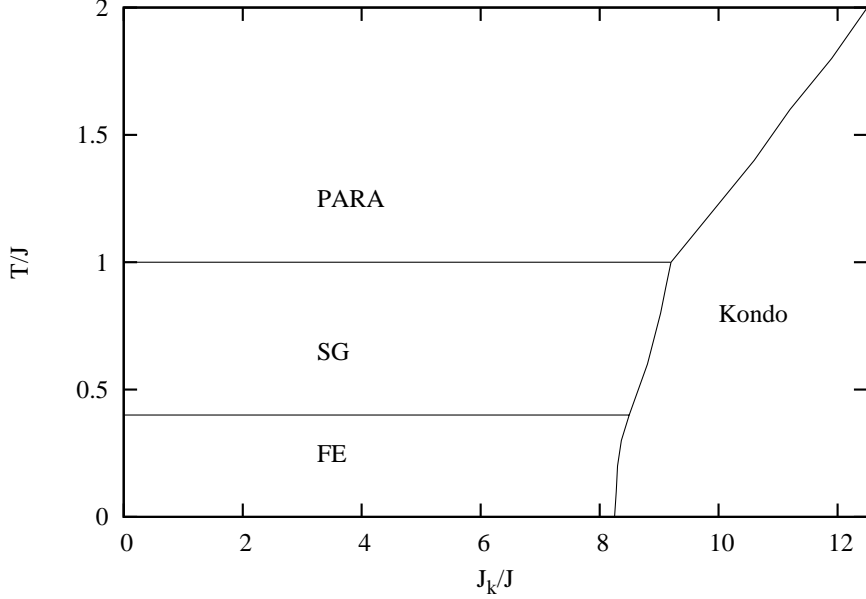


Figure 1: Phase diagram T/J versus J_K/J for $J_0/J = 1.6$ and $\Gamma/J = 0$.

with

$$H = \beta \sqrt{[2J(\eta q_2 + \xi q_1) + 2J_0 m]^2 + \Gamma^2}. \quad (21)$$

In Eq. (20), the sums over the Matsubara frequencies and over \vec{k} have been done in a way similar to Ref. [10]. We have also used here the usual approximation of a constant density of states for the d electrons, $\rho = \frac{1}{2D}$ for $-D < \epsilon < D$. The use of this density of states allows a direct comparison of phase diagrams obtained in this work with previous ones given in Refs. [10, 11, 16]. Finally, assuming that the probability distribution $P(\xi, \eta) = P(\xi)P(\eta)$, we can compute $\langle\langle \dots \rangle\rangle_{\xi\eta}$ in Eq. (20) using Eqs. (3) and (19).

3 Numerical results

The coupled saddle point equations for q_1 , q_2 , m and λ can be obtained directly from Eqs. (20)-(21). The numerical solutions for such order parameters allow us to obtain the following phases: (i) paramagnetism (PARA) given by $q_1 = q_2 = 0$, $m = 0$ and $\lambda = 0$; (ii) the SG phase given by $q_1 = q_2 \neq 0$, $m = 0$ and $\lambda = 0$; (iii) the mixed phase (SG+FE) given by $q_1 = q_2 \neq 0$, $m \neq 0$ and $\lambda = 0$; (iv) ferromagnetism (FE) given by $q_1 = q_2 = 0$, $m \neq 0$ and $\lambda = 0$; (v) Kondo state where only λ is different from zero. For numerical results, $D/J = 12$ is used.

Phase diagrams giving temperature T versus J_K (in units of J) can be built for several values of J_0/J and Γ/J . In Figure (1), such a phase diagram is displayed for $J_0/J = 1.6$ and $\Gamma/J = 0$. For this case, in the large J_K region there is only one solution which corresponds to the Kondo state. When J_K decreases, the Kondo solution disappears. Actually, it is substituted by the magnetic solutions PARA, SG and FE which appear in that order when T is

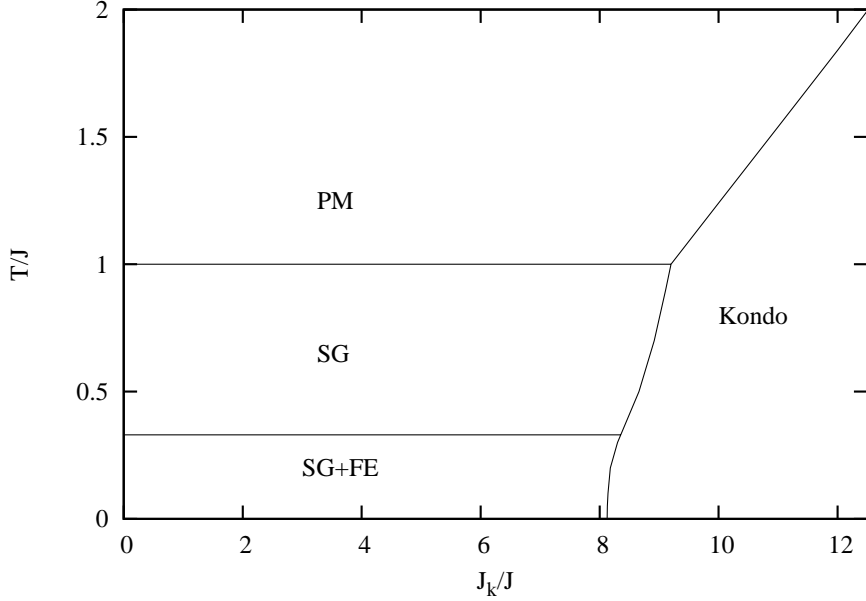


Figure 2: Phase diagram T/J versus J_K/J for $J_0/J = 1.3$ and $\Gamma/J = 0$.

lowered. In Figure (2), we take $J_0/J = 1.3$ and $\Gamma = 0$. This decrease of J_0/J from 1.6 to 1.3 does not affect the Kondo state, but changes a lot the magnetic solutions. In Figure (2), the solution FE is replaced by the mixed phase SG+FE, while the size of the region where the SG solution exists remains almost the same as in Figure (1). In Figure (3), the transverse field Γ is maintained equal to 0 and we take an intermediate value $J_0/J = 1.4$. As in the two previous cases, the Kondo state is not really affected in the large J_K region, but the region of the magnetic solutions in the phase diagram is again modified. Besides the existence of SG and SG+FE solutions, when the temperature is decreased, there is also an additional FE solution at much lower temperatures. In other words, in a small range of J_0/J ($1.3 \leq J_0/J \leq 1.6$), the phase diagrams present several scenarios concerning the existence of magnetic solutions. In contrast, the Kondo state is robust to such changes of J_0/J .

Furthermore, a new situation is obtained when the transverse field is turned on, as can be seen in Figure (4). For instance, for $\Gamma = 1.0$, the Kondo solution is obtained for a value of J_K/J a little larger than that found previously for $\Gamma = 0.4$ or $\Gamma = 0$ and simultaneously, the range of J_K/J where the magnetic solutions are found is increased. Moreover, for such a decrease of Γ from 1 to 0, the transition temperatures between the magnetic phases are clearly depressed. But the most important feature observed with the increase of Γ concerns the magnetic solutions, because the SG+FE and FE phases disappear completely and it remains only the SG phase for a sufficiently large Γ value.

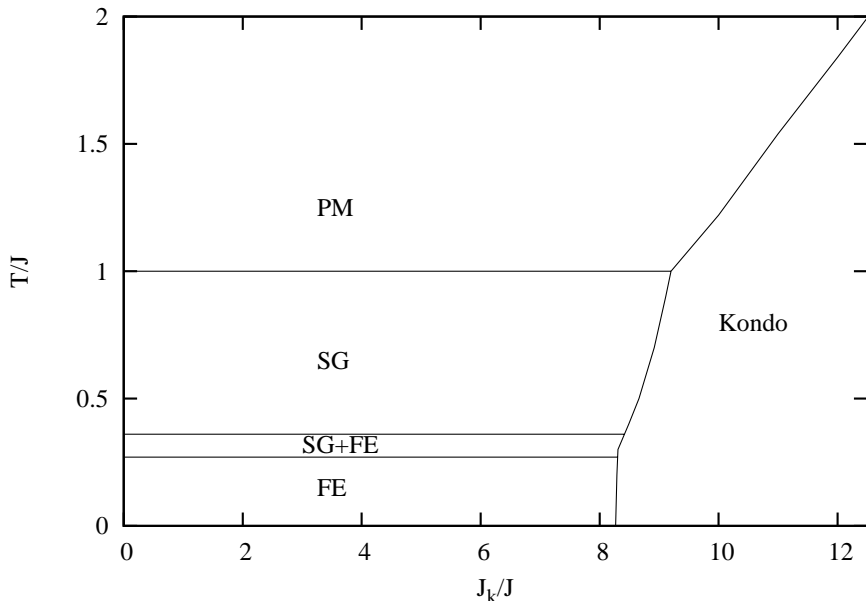


Figure 3: Phase diagram T/J versus J_K/J for $J_0/J = 1.4$ and $\Gamma/J = 0$.

4 Conclusions

In the present work, the KIL model has been studied with assuming that the inter-site spin coupling J_{ij} between localized spins is a random coupling given by the van Hemmen model as given in Eq. (2). It has also been added to the model a transverse field Γ which mimics a Heisenberg spin-flipping term.

The results are shown in Figures (1)-(4). For $\Gamma = 0$, they basically display two regimes when the strength J_K of the Kondo interaction is varied in units of the component J of the coupling J_{ij} (see Eq. (2)). In the first regime obtained for large J_K values, there is only the Kondo phase. In contrast, the second regime with only the magnetic solutions SG, SG+FE and FE exists when J_K is decreased. One important point is the order in which the magnetic phases are found when the temperature is decreased. For instance, the SG phase is found at higher temperature. Then, it can appear a SG+FE phase. The pure FE phase is found only at the lowest temperatures. It is also important to notice that the existence of the different solutions SG, SG + FE or FE depends on the strength of the ferromagnetic component J_0 (given in units of J) of the coupling J_{ij} , as can be seen in the Figures (1)-(3). When Γ is different from zero, the two regimes discussed previously are affected. While the Kondo solution needs larger values of J_K to be found, the magnetic solutions found at lower temperatures disappear rapidly when Γ is increased.

It should be emphasized that the present approach using the J_{ij} coupling given by the vH model yields two important improvements with respect to previous approaches. The first one concerns the use of the replica method which is not necessary here to generate the thermodynamics. This is an important improvement with respect to the previous approaches using the bond disorder

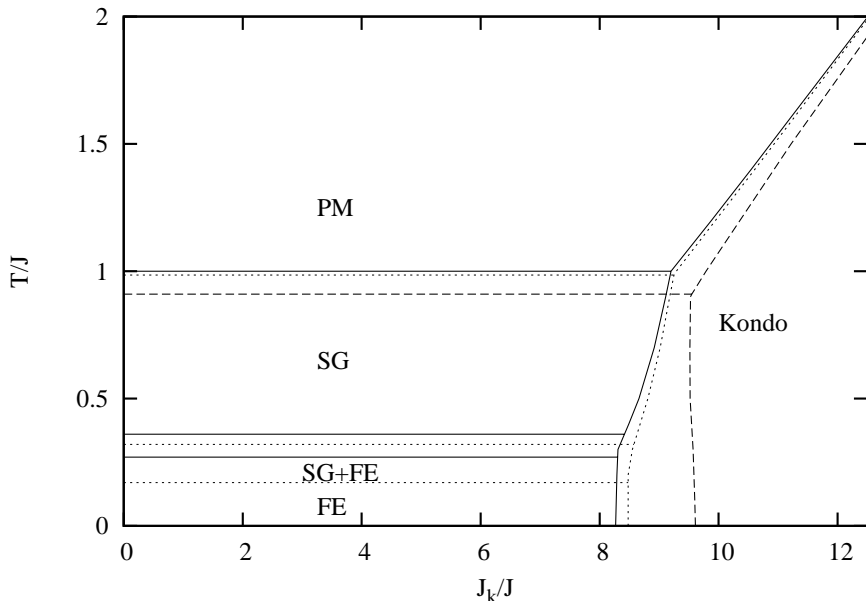


Figure 4: Phase diagrams T/J versus J_K/J for $J_0/J = 1.4$ and three values of Γ/J : 0, 0.4 and 1.0. The dashed, dotted and full lines are results for $\Gamma/J = 1.0$, $\Gamma/J = 0.4$ and $\Gamma/J = 0.0$, respectively. The critical lines for $\Gamma/J = 0$ occur at higher temperatures than those ones for $\Gamma/J = 0.4$ and $\Gamma/J = 1.0$. In particular, for $\Gamma/J = 1.0$ there is no more SG+FE and FE solutions.

given by the SK-like Gaussian random J_{ij} in the KIL model [10, 21, 12, 14, 11] or using the previous Mattis-like approach [16]. For instance, the presence of magnetic solutions in these approaches is quite dependent on which particular scheme of replica solution is used, as explained in the discussion of Ref. [25].

As our present results suggest, the second improvement concerns the particular kind of site disorder given by the vH model introduced in the KIL model with a certain range of J_0 , which allows to obtain magnetic solutions SG, SG+FE and FE phases when the temperature is decreased. In that sense, the weakness of the approach proposed in Reference [16] is overcome and we are able to introduce here a mixed phase SG+FE.

Thus, our present calculation using the van Hemmen site disorder can describe Cerium disordered physical systems such as $CeNi_{1-x}Cu_x$ or $CePd_{1-x}Rh_x$ alloys. In particular, Figures 3 and 4 can describe the phase diagram of $CeNi_{1-x}Cu_x$ with J_K increasing with an increasing Nickel concentration, by explaining the Kondo behavior observed for x close to 1 and by proposing a good interpretation of the complicate magnetic behavior observed for smaller x values. These are indications that the use of the van Hemmen site disorder could be useful to describe physical systems such as $CeNi_{1-x}Cu_x$ or $CePd_{1-x}Rh_x$ alloys, although the low temperature phase in these alloys is a Kondo-cluster-glass followed by a disordered ferromagnetic one. However, it is important to notice that canonical spins have been used in the present work. This description is obviously not sufficient to capture the complexity of the cluster glass state. However, earlier

results for a mean field formulation of the cluster glass indicate that there are no essential differences between canonical spins and clusters of spins, as far as the phase boundaries are concerned [26]. One can, therefore, expect that most of the previous discussion concerning the sequence of magnetic orders as a function of J_K can be preserved even if the problem is formulated in terms of clusters of spins instead of canonical spins as it is done in the present work.

On the other hand, we are presently working on a theoretical description of the Kondo-Cluster-Glass, by solving exactly the problem in a small cluster with n_s atoms interacting between them by a disorder spin glass-like interaction. We have already solved the problem with only $n_s = 3$ and a disorder intercluster bonding given by the Sherrington-Kirkpatrick interaction [27]. We think that the van Hemmen approach is easier to treat and we are presently working on clusters with a larger number n_s , in order to have finally a more local description of the Kondo-Cluster-Glass observed in some disordered Kondo Cerium systems.

In conclusion, we have to remark that our van Hemmen-Kondo description yields considerable improvements with respect to previous theoretical models in the two following points, the non consideration of the replica method and the problem of the mixed SG+FE phase. The validity of the van Hemmen model, which does not use the replica trick method, has been discussed in detail and it has been shown that this model is perfectly able to describe the spin glass experiments and that it is simpler than the other models for a mathematical treatment [28, 29]. On the other side, our van Hemmen-Kondo model gives with decreasing temperature a SG phase, a SG+FE one and finally a ferromagnetic phase and the intermediate SG+FE phase is a real mixed phase with together non zero SG and FE order parameters. This model gives a good account for the experimental phase diagrams of disordered Cerium systems, such as $CeNi_{1-x}Cu_x$ alloys, and can be used to have a more local description of the Kondo-Cluster-Glass phase.

Acknowledgments

B. Coqblin acknowledges the European Cost P16 Action for financial support. S.G. Magalhaes and F.M. Zimmer acknowledge the CNPq for financial support.

Appendix

In this appendix, we present in details the procedure which allows to introduce the SG and FE order parameters in the problem. First, the random component of J_{ij} given in Eq. (2) can be rewritten as:

$$\begin{aligned} & \frac{\beta J}{N} \sum_{i \neq j} (\eta_i \xi_j + \xi_i \eta_j) S_i^z S_j^z = \\ & \frac{\beta J}{N} \left[\sum_{j=1}^N (\eta_j + \xi_j) S_i^z \right]^2 - \frac{\beta J}{N} \left[\sum_{j=1}^N \eta_j S_i^z \right]^2 \\ & - \frac{\beta J}{N} \left[\sum_{j=1}^N \xi_j S_i^z \right]^2 - \frac{2\beta J}{N} \sum_{j=1}^N (\eta_j S_i^z)(\xi_j S_i^z) \end{aligned} \quad (22)$$

while the ferromagnetic one is

$$\frac{\beta J_0}{N} \sum_{i \neq j} S_i^z S_j^z = \frac{\beta J_0}{N} \left[\sum_i S_i^z \right]^2 - \frac{J_0}{N} \sum_i (S_i^z)^2. \quad (23)$$

The last terms in Eqs (22) and (23) vanish in the thermodynamic limit.

The Hubbard-Stratonovich transformation can be used to linearize the action A_{vH}^{stat} . Thus Z_{eff} in Eq. (12) becomes:

$$Z_{eff} = \left(\frac{N}{2\pi} \right)^2 \int_{-\infty}^{+\infty} d\bar{q}_1 \int_{-\infty}^{+\infty} d\bar{q}_2 \int_{-\infty}^{+\infty} d\bar{q}_3 \times \int_{-\infty}^{+\infty} dm \exp \left(-\frac{N}{2} (\bar{q}_1^2 + \bar{q}_2^2 + \bar{q}_3^2) - \frac{N\bar{m}^2}{2} + \ln \Lambda(\bar{q}_1, \bar{q}_2, \bar{q}_3, \bar{m}) \right) \quad (24)$$

where the function $\Lambda(\bar{q}_1, \bar{q}_2, \bar{q}_3, \bar{m})$ in Eq.(24) is:

$$\Lambda(q_1, q_2, q_3, m) = \int D(\psi^* \psi) \exp \left(\sum_{i,\sigma} \sum_{\omega} \underline{\psi}_{i\sigma}^* \underline{G}_{ij}^{-1}(\omega|h_j) \underline{\psi}_{j\sigma}(\omega) \right) \quad (25)$$

with:

$$\underline{G}_{ij}(\omega|h_j) = [(i\omega + \beta\epsilon_0)\underline{I} - \underline{\sigma}_z h_j + \beta\Gamma\underline{\sigma}_x] \delta_{ij} - \frac{\beta^2 J_k^2 \lambda^2}{i(\omega + \mu_d)\delta_{ij} - \beta t_{ij}} \underline{I}. \quad (26)$$

The random field in Eq.(26) is

$$h_j = \sqrt{2\beta J} (i\eta_j \bar{q}_1 + i\xi_j \bar{q}_2 + (\eta_j + \xi_j) \bar{q}_3) + \sqrt{2\beta J_0} \bar{m} \quad (27)$$

The saddle point solution of Eq. (24) gives:

$$\bar{q}_1 = i\sqrt{\beta J} \frac{1}{N} \sum_j \langle \xi_j S_j^z \rangle = i\sqrt{2\beta J} q_1 \quad (28)$$

$$\bar{q}_2 = i\sqrt{\beta J} \frac{1}{N} \sum_j \langle \eta_j S_j^z \rangle = i\sqrt{2\beta J} q_2 \quad (29)$$

$$\bar{q}_3 = \sqrt{2\beta J} (q_1 + q_2) \quad (30)$$

and

$$\bar{m} = \sqrt{2\beta J_0} \frac{1}{N} \sum_j \langle S_j^z \rangle = \sqrt{2\beta J_0} m \quad (31)$$

The symbol $\langle \dots \rangle$ is the thermodynamical average and $i^2 = -1$ in Eqs. (28)-(31). The integral over the Grassmann fields can be performed in Eq.(25), leading to:

$$\Lambda(q_1, q_2, m) = \exp \left(\sum_{\omega} \ln(\det \underline{G}_{ij}^{-1}(\omega|h_j)) \right). \quad (32)$$

References

- [1] B. Coqblin, M. D. Nunez-Regueiro, A. Theumann, J. R. Iglesias, S. G. Magalhaes, *Philosophical Magazine* **86**, 2576 (2006).
- [2] E. Miranda, V. Dobrosavljevic, *Rep. Prog. Phys.* **68**, 2337 (2005).
- [3] S. Majundar, E. V. Sampathkumuran, St. Berger, M. Della Mea, H. Michor, E. Bauer, M. Brando, J. Hemberger, A. Loidl, *Solid State Comm.*, **121** 665 (2002).
- [4] T. Westerkamp, M. Deppe, R. Kuchler, M. Brando, C. Geibel, P. Gegenwart, A. P. Pikul, F. Steglich, *Phys. Rev. Lett.* **102**, 206404 (2009).
- [5] T. Westerkamp, M. Brando, N. Caroca-Canales, M. Deppe, P. Gegenwart, C. Geibel, R. Kuchler, A. P. Pikul, J.G. Sereni, F. Steglich, to be published in the Proceedings of ICM 2009, arXiv:0910.5840v1
- [6] N. Marcano, J. I. Espeso, J. C. Gomez Sal, J. Rodriguez Fernandez, J. Herrero Albillos and F. Bartolome, *Phys. Rev.* **71**, 134401 (2005).
- [7] N. Marcano, J. C. Gomez Sal, J. I. Espeso, L. Fernandez Barquin, C. Paulsen, *Phys. Rev.* **76**, 224419 (2007).
- [8] J. Garcia Soldevilla, J. C. Gomez Sal, J. A. Blanco, J. I. Espeso, J. Rodriguez Fernandez, *Phys. Rev.* **61**, 6821 (2000).
- [9] A. P. Pikul, N. Caroca-Canales, M. Deppe, P. Gegenwart, J.G. Sereni, C. Geibel, F. Steglich, *J. Phys.: Condens. Matter* **18**, L535 (2006).
- [10] A. Theumann, B. Coqblin, S. G. Magalhaes, A. A. Schmidt, *Phys. Rev. B* **63**, 054409 (2001).
- [11] S. G. Magalhaes, A. A. Schmidt, A. Theumann, B. Coqblin, *Eur. Phys. J. B* **30**, 419 (2002).
- [12] S. G. Magalhaes, A. A. Schmidt, F. M. Zimmer, A. Theumann, B. Coqblin, *Eur. Phys. J. B* **34**, 447 (2003).
- [13] A. J. Bray, M. A. Moore, *J. Phys. C* **13**, L655 (1980).
- [14] S. G. Magalhaes, F. M. Zimmer, B. Coqblin, *J. Phys.: Condens. Matter* **18**, 3479 (2006).
- [15] S. Kirkpatrick, D. Sherrington, *Phys. Rev. B* **17**, 4384 (1978).
- [16] S. G. Magalhaes, F. M. Zimmer, P. R. Krebs, B. Coqblin, *Phys. Rev. B* **74**, 014427 (2006).
- [17] D. J. Mattis, *Phys. Lett.* **56A**, 421 (1977).
- [18] D. J. Amit, *Modelling Brain Function. The world of Attractor Neural Networks* (Cambridge University Press, Cambridge, England, 1989).
- [19] J. L. van Hemmen, *Phys. Rev. Lett.* **49**, 409 (1982).
- [20] J. R. Viana, Y. Nogueira, J. R. de Sousa, *Phys. Rev. B* **66**, 113307 (2002).

- [21] A. Theumann, B. Coqblin, Phys. Rev. B **69**, 214418 (2004).
- [22] K. Binder, A. P. Young, Review of Modern Physics **58**, 801 (1986).
- [23] J. R. L. de Almeida, D. J. Thouless, J. Phys. A **11**, 983 (1978).
- [24] G. Parisi, J. Phys. **13**, 1101 (1980).
- [25] S. G. Magalhaes, F. M. Zimmer, B. Coqblin, Physica B **378-380**, 131 (2006).
- [26] C. M. Soukoulis, K. Levin, Phys. Rev. B **18**, 1439 (1978).
- [27] F. M. Zimmer, S. G. Magalhaes, B. Coqblin, Physica B **404**, 2972 (2009).
- [28] T. C. Choy, D. Sherrington, J. Phys. C: Solid State Phys. **19**, 739 (1984).
- [29] J. L. van Hemmen, J. Phys. C: Solid State Phys. **19**, L379 (1986).